EUROPEAN ORGANIZATION FOR NUCLEAR RESEARCH

CERN-EP/2003-072
November 12, 2003

Study of Spin and Decay-Plane Correlations of W Bosons in the $e^+e^- \to W^+W^-$ Process at LEP

The L3 Collaboration

Abstract

Data collected at LEP at centre-of-mass energies $\sqrt{s} = 189 - 209$ GeV are used to study correlations of the spin of W bosons using $e^+e^- \to W^+W^- \to \ell\nu q\bar{q}$ events. Spin correlations are favoured by data, and found to agree with the Standard Model predictions. In addition, correlations between the W-boson decay planes are studied in $e^+e^- \to W^+W^- \to \ell\nu q\bar{q}$ and $e^+e^- \to W^+W^- \to q\bar{q}q\bar{q}$ events. Decay-plane correlations are measured to be consistent with the Standard Model predictions.

Submitted to *Eur. Phys. Jour. C*

Introduction

The study of the properties of the W boson constitutes one of the main physics goals of the LEP experiments. We have previously reported on the measurement of the helicity fractions of W bosons in $e^+e^- \to W^+W^- \to \ell\nu q\bar{q}$ events, with ℓ denoting either an electron or a muon, using data collected at LEP at centre-of-mass energies, $\sqrt{s}$, up to 209 GeV [1]. Measurements of W-boson polarisation were also reported in the framework of a spin-density matrix analysis [2]. The same data sample is used here to study correlations of the spin of W bosons as well as correlations between the decay planes of the two W bosons. This last study also includes $e^+e^- \to W^+W^- \to q\bar{q}q\bar{q}$ events. Some correlations of the spin of W bosons in the $e^+e^- \to W^+W^-$ process are expected in the Standard Model and are accessible with the size of the data sample collected at LEP. Weak decay plane correlations are also expected.

Studies of triple-gauge-couplings of the W boson [3], which rely on the analysis of the full differential cross section of the $e^+e^- \to W^+W^-$ process, have an implicit sensitivity to these correlations. Their results are presented in terms of couplings describing the Lorentz-invariant γWW and ZWW vertices. The aim of the analysis presented in this Article, as a natural extension of the work of Reference 1, is a direct and model independent measurement of the spin and decay-plane correlations. This enables a specific test of the corresponding Standard Model predictions, as suggested in References 4 and 5 for the spin and decay-plane correlations, respectively. Large deviations from the Standard Model predictions, possibly outside the reach of LEP, would suggest anomalous mechanisms for W-boson pair-production in e^+e^- collisions such as one-loop contributions from new particles or in general effects from any model with a symmetry breaking mechanism which affects interactions of longitudinally-polarised W bosons. To date, no such direct measurement was reported and this study introduces a new technique which could be exploited at future high-luminosity lepton colliders.

W-boson spin correlations are measured in $e^+e^- \to W^+W^- \to \ell\nu q\bar{q}$ events by tagging the helicity of the W boson which decays into hadrons and measuring the helicity of the W boson which decays into leptons. We consider two subsamples of W-boson pairs: the first is enriched in events where W^- bosons decaying into hadrons have a helicity $\lambda_{W^-} = \pm 1$ and the second is depleted of these events [1)]. A difference in the helicity compositions of the W bosons decaying into leptons for the two subsamples would indicate the presence of W-boson spin correlations.

The helicity fractions of the W^- boson decaying into leptons are obtained in a model independent approach from the shape of the distribution of the polar decay angle, θ^*_ℓ, between the charged lepton and the W^--boson flight direction in the W^--boson rest frame. The differential distribution of leptonic W^--boson decays is:

$$\frac{1}{N}\frac{\mathrm{d}N}{\mathrm{d}\cos\theta^*_\ell} = f_-\frac{3}{8}\,(1+\cos\theta^*_\ell)^2 + f_+\frac{3}{8}\,(1-\cos\theta^*_\ell)^2 + f_0\frac{3}{4}\sin^2\theta^*_\ell, \tag{1}$$

where f_-, f_+ and f_0 represent the fractions of W^- bosons in the -1, $+1$ and 0 helicity states, respectively. Assuming CP invariance, these equal the fractions of the corresponding helicity states $+1$, -1 and 0 of the W^+ boson. For hadronic W-boson decays, considering only the absolute value of the cosine of the polar decay angle, $|\cos\theta^*_\mathrm{q}|$, the differential distribution is:

$$\frac{1}{N}\frac{\mathrm{d}N}{\mathrm{d}|\cos\theta^*_\mathrm{q}|} = f_\pm\frac{3}{4}(1+|\cos\theta^*_\mathrm{q}|^2) + f_0\frac{3}{2}(1-|\cos\theta^*_\mathrm{q}|^2), \tag{2}$$

[1)] The charge conjugate state W^+ is also included throughout this Article. CP conservation is assumed, as verified in W-boson polarisation studies [1, 2].

with $f_{\pm}$=f_{+}+f_{-}. It is worthwhile to remark that the only hypothesis in the derivation of Equations 1 and 2 is the decay of a unit-spin W boson into fermions.

The values of f_{-}, f_{+} and f_{0} are a function of $\sqrt{s}$ and the W^{-}-boson production angle with respect to the incoming e^{-}, $\cos\Theta_{\mathrm{W}^{-}}$. The numerical values corresponding to the data sample investigated in this Article are therefore dependent on the integrated luminosity collected at each centre-of-mass energy at which the LEP collider was operated.

The fractions of helicity combinations $(\lambda_{\mathrm{W}^{-}}, \lambda_{\mathrm{W}^{+}})$ depend strongly on $\cos\Theta_{\mathrm{W}^{-}}$. As an example, Figure 1 shows the results of a leading-order analytical calculation [6]. This property is used to select intervals in which a particular helicity combination is enriched and thus spin correlations are more significant. Two intervals are considered: the forward bin, $0.3 < \cos\Theta_{\mathrm{W}^{-}} < 0.9$, where the fraction of the helicity combination $(\lambda_{\mathrm{W}^{-}}, \lambda_{\mathrm{W}^{+}}) = (-1, +1)$ is increased to about 68% of all W-boson pairs, compared to an average value of 49% over the whole $\cos\Theta_{\mathrm{W}^{-}}$ range; and the backward bin, $-0.9 < \cos\Theta_{\mathrm{W}^{-}} < -0.3$, where the fraction of the helicity combination $(\lambda_{\mathrm{W}^{-}}, \lambda_{\mathrm{W}^{+}}) = (0, 0)$ is increased to about 26%, compared to an average value of 8%.

To tag the helicity of the W boson which decays into hadrons, cuts on $|\cos\theta^{*}_{\mathrm{q}}|$ are used. According to Equation 2, for small values of $|\cos\theta^{*}_{\mathrm{q}}|$, the sample is depleted of helicity ±1 states, while for large values of $|\cos\theta^{*}_{\mathrm{q}}|$ the sample is enriched in helicity ±1 states, as shown in Figure 2. The interval $|\cos\theta^{*}_{\mathrm{q}}| < 0.33$ is chosen for the $\lambda_{\mathrm{W}^{-}} = \pm1$ depleted sample and the interval $|\cos\theta^{*}_{\mathrm{q}}| > 0.66$ for the $\lambda_{\mathrm{W}^{-}} = \pm1$ enriched sample. The helicity fractions of the W^{-} bosons decaying into leptons are obtained from a fit of Equation 1 to the distribution of $\cos\theta^{*}_{\ell}$ [7].

Decay-plane correlations are studied in both $\mathrm{e^{+}e^{-}} \to \mathrm{W^{+}W^{-}} \to \ell\nu\mathrm{q\bar{q}}$ and $\mathrm{e^{+}e^{-}} \to \mathrm{W^{+}W^{-}} \to \mathrm{q\bar{q}q\bar{q}}$ events using the absolute value of the angle, $|\Delta\phi|$, between the planes defined by the decay products of the two W bosons in the rest frame of the W-boson pair. The strength of the correlation is measured by the parameter D of the differential distribution [8]:

$$\frac{1}{N}\frac{\mathrm{d}N}{\mathrm{d}\,|\Delta\phi|} = 1 + D\cos 2\,|\Delta\phi|\,. \tag{3}$$

The experimental distribution of $|\Delta\phi|$ is fitted to obtain the parameter D [7]. The expected value of D in the Standard Model, for the $\sqrt{s}$ range under investigation, is estimated with a leading-order analytical calculation [8] to vary from 0.021 at $\sqrt{s} = 189$ GeV to 0.015 at $\sqrt{s} = 209$ GeV, with a luminosity-weighted average of 0.018.

For both analyses, prior to the fits, the distributions of the measured angles are corrected by means of an efficiency correction function which accounts for selection efficiencies, migration effects and the presence of initial state radiation. This correction function is obtained from large Monte Carlo samples as the ratio of the angular distributions for simulated and generated events.

Data and Monte Carlo Samples

The analysis is based on $629.3\,\mathrm{pb}^{-1}$ of data collected with the L3 detector [9] at $\sqrt{s} = 189 - 209$ GeV, as detailed in Table 1, corresponding to a luminosity-weighted average $\sqrt{s}$ value of 197.9 GeV.

Signal Monte Carlo events are generated using the KORALW [10] program for the $\mathrm{e^{+}e^{-}} \to \mathrm{W^{+}W^{-}} \to \mathrm{e}\nu\mathrm{q\bar{q}}, \mu\nu\mathrm{q\bar{q}}$ and $\mathrm{q\bar{q}q\bar{q}}$ processes. The Standard Model predictions for the W-boson spin correlations and the decay-plane correlations are obtained from the distributions generated

at different values of $\sqrt{s}$, combined according to the collected luminosity. Background processes are generated using KORALW for all other final states of W-boson pair-production, KK2f [11] for the $e^+e^- \to q\bar{q}(\gamma)$ process, and PYTHIA [12] for the $e^+e^- \to ZZ$ process. For studies of systematic effects, signal events are also generated using the EEWW [13], YFSWW [14] and EXCALIBUR [15] programs.

To test the consistency of the predictions for W-boson spin and decay-plane correlations, large samples of signal events are generated using the EEWW and YFSWW Monte Carlo programs. These differ from KORALW in the level and implementation of $\mathcal{O}(\alpha)$ corrections. The predictions given by the three programs for the strength of the correlations are in agreement with each other, within their own statistical uncertainties.

The predicted Standard Model value of the parameter D, which describes the decay-plane correlations is $D = 0.010 \pm 0.002$, as obtained with the KORALW Monte Carlo. The uncertainty is statistical. This differs from the value $D = 0.018$ obtained by an analytical calculation [8] due to the inclusion of radiative effects in the Monte Carlo.

The L3 detector response is simulated with the GEANT [16] and GHEISHA [17] packages. Detector inefficiencies, as monitored during the data taking periods, are included.

After detector simulation, the average resolution on $\cos\Theta_{W^-}$ is found to be 0.06 while the resolution on $\cos\theta^*$ is found to be 0.10 for electrons, 0.11 for muons and 0.14 for hadrons. The resolution on $|\Delta\phi|$ is 7.5° for semi-leptonic events and 10.0° for hadronic events.

Event Selection

The selection of $e^+e^- \to W^+W^- \to \ell\nu q\bar{q}$ events is the same as for the study of the W-boson polarisation [1], however, the low-statistics data sample collected at $\sqrt{s} = 183$ GeV is not considered here. The numbers of selected events are listed in Table 1 for different values of $\sqrt{s}$. In total, 1861 events are selected with an average efficiency of 67.6% and an average purity of 96.6%, which are only slightly dependent on $\sqrt{s}$. The contamination from the $e^+e^- \to W^+W^- \to \tau\nu q\bar{q}$ and $e^+e^- \to q\bar{q}(\gamma)$ processes is 2.3% and 1.1%, respectively.

The selection of $e^+e^- \to W^+W^- \to q\bar{q}q\bar{q}$ events is performed as follows. High multiplicity events are selected by requiring more than 20 charged tracks and more than 25 calorimetric clusters. The visible energy of the event must satisfy $E_{\rm vis} > 0.75\sqrt{s}$. To reject the $e^+e^- \to q\bar{q}(\gamma)$ background, the event thrust must be less than 0.88 and the polar angle of the thrust axis, θ_T, has to satisfy $|\cos\theta_T| < 0.95$. The missing momentum of the event has to be less than 60 GeV. Events containing electrons, muons or photons with energy greater than 20, 20 or 40 GeV, respectively, are rejected. Jets are reconstructed using the Durham algorithm [18], with a jet-resolution parameter for which the event changes from a four-jet into a three-jet topology, y_{34}, greater than 0.0015. Two pairs of jets are formed, corresponding to two W bosons. Of the three combinations, the optimal pairing of jets is chosen as the one with the smallest mass difference, disregarding the pairing corresponding to the smallest mass sum. This algorithm yields the correct assignment of jets to W bosons for about 70% of the selected Monte Carlo events. Finally, the reconstructed W bosons must have a mass between 40 and 120 GeV. Figure 3 shows the distributions of some selection variables for data and Monte Carlo.

The numbers of events selected by these criteria at different values of $\sqrt{s}$ are listed in Table 1. In total, 4919 events are selected with an average efficiency of 76.3% and an average purity of 75.7%, which do not strongly depend on $\sqrt{s}$. The background contamination is 18.9% from the $e^+e^- \to q\bar{q}(\gamma)$ process, 4.9% from the $e^+e^- \to ZZ$ process and 0.5% from W-boson pairs which decay into other final states.

Analysis of W-Boson Spin Correlations

The values of $\cos\theta^*_\ell$ and $|\cos\theta^*_{\rm q}|$ are determined for each selected event. The latter is approximated by the absolute value of the cosine of the angle of the thrust axis of the W-boson decaying into hadrons, calculated with respect to the W-boson flight direction in the W-boson rest frame.

The W-pair events are then classified according to the values of $\cos\Theta_{\rm W^-}$ and $|\cos\theta^*_{\rm q}|$ to build four test samples:

$$0.3 < \cos\Theta_{\rm W^-} < \ \ 0.9,\ |\cos\theta^*_{\rm q}| < 0.33\ ; \qquad 0.3 < \cos\Theta_{\rm W^-} < \ \ 0.9,\ |\cos\theta^*_{\rm q}| > 0.66\ ;$$

$$-0.9 < \cos\Theta_{\rm W^-} < -0.3,\ |\cos\theta^*_{\rm q}| < 0.33\ ; \quad -0.9 < \cos\Theta_{\rm W^-} < -0.3,\ |\cos\theta^*_{\rm q}| > 0.66\ .$$

In each of the samples, the fractions of W-boson helicity states for W bosons decaying into leptons are obtained from the event distributions, $\mathrm{d}N/\mathrm{d}\cos\theta^*_\ell$. For each energy point the background, as obtained from Monte Carlo simulations, is subtracted from the data. The corrected decay angle distributions at different values of $\sqrt{s}$ are combined into single distributions, shown in Figure 4, which are then fitted with the function in Equation 1, using f_- and f_0 as the fit parameters. The fraction f_+ is obtained by constraining the sum of all three parameters to unity.

Finally, the fitted fractions are corrected for the bias which originates from migration effects due to detector resolution [1, 19]. Bias correction functions are determined in each of the investigated $\cos\Theta_{\rm W^-}$ and $|\cos\theta^*_{\rm q}|$ ranges. They vary from 1% to 15%.

Several sources of systematic uncertainty are considered, as summarised in Table 2 for the measurement of the helicity fractions f_- and f_0 for all bins of $\cos\Theta_{\rm W^-}$ and $|\cos\theta^*_{\rm q}|$. All selection cuts are varied over a range of one standard deviation of the corresponding reconstruction accuracy. The corresponding variation of the helicity fractions, corrected for its statistical component, is taken as systematics. All fits are repeated with one bin more or one bin less in the angular distributions. The average difference is retained as systematics. Uncertainties on the bias and the efficiency corrections are determined by varying the bias correction function and the efficiencies in each bin by one standard deviation, as derived from the statistics of the corresponding Monte Carlo samples. Additional contamination from the non double-resonant four-fermion final states is evaluated using the EXCALIBUR Monte Carlo. Background levels are varied according to Monte Carlo statistics for the background processes.

The results of the fits are summarised in Table 3. The correlation coefficients of the parameters f_- and f_0 derived from the fit are shown in Table 4. W-boson spin correlations would manifest as sizable differences between the values of f_- and f_0 measured for the samples depleted of and enriched in ±1 helicity, respectively. These differences are also listed in Table 3. There is a general agreement between the observations and the expectation. The largest difference is observed for f_- in the forward bin, with an observation of -0.32 ± 0.12 to be compared with a prediction of -0.11 ± 0.01. Two consistency tests are performed. In the first, only data is considered and a confidence level is calculated for the absence of W-boson spin correlations. This confidence level is 1.2%, which allows to conclude that W-boson spin correlations are observed. A second test compares the data with the Standard Model KORALW Monte Carlo. The confidence level for their compatibility is 34.7%.

Analysis of Decay-Plane Correlations

Events from the $e^+e^- \to W^+W^- \to \ell\nu q\bar{q}$ and $e^+e^- \to W^+W^- \to q\bar{q}q\bar{q}$ processes are used to study correlations between the W-boson decay planes.

For $e^+e^- \to W^+W^- \to \ell\nu q\bar{q}$ events, the neutrino momentum is derived from the total missing momentum of the event. The decay plane of the W boson decaying into leptons is determined from the lepton and the neutrino directions. The decay plane of the W boson decaying into hadrons is determined from its thrust axis in the W-boson rest frame and the W-boson flight direction. For $e^+e^- \to W^+W^- \to q\bar{q}q\bar{q}$ events the reconstructed jets are boosted into the W-pair rest frame and the decay planes are determined by the two jets assigned to each reconstructed W boson. The angle $|\Delta\phi|$ between the decay planes of the two W bosons is then calculated. For each value of $\sqrt{s}$, the $|\Delta\phi|$ distribution is corrected for efficiency and background, taking also into account wrongly-paired four-jet events. The efficiency corrections are found to be basically independent from the values of D. The corrected distributions are combined into a single distribution, shown in Figure 5. A binned fit for D, using Equation 3, is performed on the normalised distribution.

The same systematic studies are performed as for the W-boson spin correlations. Additionally, for $e^+e^- \to W^+W^- \to q\bar{q}q\bar{q}$ events, several pairing algorithms are used as a cross-check. The largest difference in the fit result between the pairing methods is taken as systematic uncertainty. To reproduce the measured four jet event rate of the $e^+e^- \to q\bar{q}(\gamma)$ background [20], the corresponding Monte Carlo is scaled by +10%. Half of the effect is retained as systematics. Table 5 summarises the systematic uncertainties in the measurement of the decay-plane correlation parameter D.

The resulting value of D for $e^+e^- \to W^+W^- \to \ell\nu q\bar{q}$ events is found to be $0.051 \pm 0.033 \pm 0.019$, where the first uncertainty is statistical and the second systematic. It is in agreement with the Standard Model prediction from the KORALW Monte Carlo of $D = 0.006 \pm 0.004$, where the error reflects the Monte Carlo statistics. For $e^+e^- \to W^+W^- \to q\bar{q}q\bar{q}$ events, D is found to be $-0.016 \pm 0.028 \pm 0.016$, in agreement with the KORALW prediction of $D = 0.013 \pm 0.003$. Combining the two decay channels, a value $D = 0.012 \pm 0.021 \pm 0.012$ is found in data, in agreement with the combined value from the Standard Model KORALW Monte Carlo of $D = 0.010 \pm 0.002$.

Summary

In conclusion, this study completes our investigation of W-boson polarisation. A new technique, which is promising for future high-luminosity electron-positron colliders, is deployed and allows to establish the existence of W-boson spin correlations. Their magnitude is found to agree with the Standard Model predictions. In addition, W-boson decay-plane correlations are studied for the first time, and no large deviations with respect to the Standard Model predictions, which could hint to New Physics, are observed.

References

[1] L3 Collab., P. Achard *et al.*, Phys. Lett. **B 557** (2003) 147.

[2] OPAL Collab., G. Abbiendi *et al.*, Eur. Phys. J. **C 19** (2001) 229; OPAL Collab., G. Abbiendi *et al.*, Phys. Lett. **B 585** (2004) 223.

[3] ALEPH Collab., A. Heister *et al.*, Eur. Phys. J. **C 21** (2001) 423; DELPHI Collab., P. Abreu *et al.*, Phys. Lett. **B 502** (2001) 9; L3 Collab., P. Achard *et al.*, Phys. Lett. **B 586** (2004) 151; OPAL Collab., G. Abbiendi *et al.*, Eur. Phys. J. **C 33** (2004) 463.

[4] M. Bilenky *et al.*, Nucl. Phys. **B 409** (1993) 22.

[5] M.J. Duncan, G.L. Kane, W.W. Repko, Phys. Rev. Lett. **55** (1985) 773.

[6] K. Hagiwara *et al.*, Nucl. Phys. **B 282** (1987) 253.

[7] R. Ofierzynski, *Measurement of the W Boson Polarisations using the L3 Detector at LEP II*, Ph.D. Thesis, ETH Zürich (2005).

[8] M.J. Duncan, G.L. Kane, W.W. Repko, Nucl. Phys. **B 272** (1986) 517.

[9] L3 Collab., B. Adeva *et al.*, Nucl. Inst. Meth. **A 289** (1990) 35; L3 Collab., O. Adriani *et al.*, Phys. Rept. **236** (1993) 1; I. C. Brock *et al.*, Nucl. Instr. and Meth. **A 381** (1996) 236; M. Chemarin *et al.*, Nucl. Inst. Meth. **A 349** (1994) 345; M. Acciarri *et al.*, Nucl. Inst. Meth. **A 351** (1994) 300; A. Adam *et al.*, Nucl. Inst. Meth. **A 383** (1996) 342; G. Basti *et al.*, Nucl. Inst. Meth. **A 374** (1996) 293.

[10] KORALW version 1.33 is used; M. Skrzypek *et al.*, Comp. Phys. Comm. **94** (1996) 216; M. Skrzypek *et al.*, Phys. Lett. **B 372** (1996) 289.

[11] KK2f version 4.12 is used; S. Jadach, B. F. L. Ward and Z. Wąs, Comp. Phys. Comm. **130** (2000) 260.

[12] PYTHIA version 5.722 is used; T. Sjöstrand, preprint CERN-TH/7112/93 (1993), revised 1995; T. Sjöstrand, Comp. Phys. Comm. **82** (1994) 74.

[13] EEWW version 1.1 is used; J. Fleischer *et al.*, Comp. Phys. Comm. **85** (1995) 29.

[14] YFSWW3 version 1.14 is used: S. Jadach *et al.*, Phys. Rev. **D 54** (1996) 5434; Phys. Lett. **B 417** (1998) 326; Phys. Rev. **D 61** (2000) 113010; Phys. Rev. **D 65** (2002) 093010.

[15] EXCALIBUR version 1.11 is used; F.A. Berends, R. Pittau and R. Kleiss, Comp. Phys. Comm. **85** (1995) 437.

[16] GEANT version 3.15 is used; R. Brun *et al.*, preprint CERN DD/EE/84-1 (1984), revised 1987.

[17] H. Fesefeldt, RWTH Aachen report PITHA 85/02 (1985).

[18] S. Catani *et al.*, Phys. Lett. **B 269** (1991) 432; S. Bethke *et al.*, Nucl. Phys. **B 370** (1992) 310.

[19] L3 Collab., M. Acciarri *et al.*, Phys. Lett. **B 474** (2000) 194.

[20] L3 Collab., M. Acciarri *et al.*, Phys. Lett. **B 496** (2000) 19.

The L3 Collaboration:

P.Achard,[20] O.Adriani,[17] M.Aguilar-Benitez,[25] J.Alcaraz,[25] G.Alemanni,[23] J.Allaby,[18] A.Aloisio,[29] M.G.Alviggi,[29] H.Anderhub,[49] V.P.Andreev,[6,34] F.Anselmo,[8] A.Arefiev,[28] T.Azemoon,[3] T.Aziz,[9] P.Bagnaia,[39] A.Bajo,[25] G.Baksay,[26] L.Baksay,[26] S.V.Baldew,[2] S.Banerjee,[9] Sw.Banerjee,[4] A.Barczyk,[49,47] R.Barillère,[18] P.Bartalini,[23] M.Basile,[8] N.Batalova,[46] R.Battiston,[33] A.Bay,[23] F.Becattini,[17] U.Becker,[13] F.Behner,[49] L.Bellucci,[17] R.Berbeco,[3] J.Berdugo,[25] P.Berges,[13] B.Bertucci,[33] B.L.Betev,[49] M.Biasini,[33] M.Biglietti,[29] A.Biland,[49] J.J.Blaising,[4] S.C.Blyth,[35] G.J.Bobbink,[2] A.Böhm,[1] L.Boldizsar,[12] B.Borgia,[39] S.Bottai,[17] D.Bourilkov,[49] M.Bourquin,[20] S.Braccini,[20] J.G.Branson,[41] F.Brochu,[4] J.D.Burger,[13] W.J.Burger,[33] X.D.Cai,[13] M.Capell,[13] G.Cara Romeo,[8] G.Carlino,[29] A.Cartacci,[17] J.Casaus,[25] F.Cavallari,[39] N.Cavallo,[36] C.Cecchi,[33] M.Cerrada,[25] M.Chamizo,[20] Y.H.Chang,[44] M.Chemarin,[24] A.Chen,[44] G.Chen,[7] G.M.Chen,[7] H.F.Chen,[22] H.S.Chen,[7] G.Chiefari,[29] L.Cifarelli,[40] F.Cindolo,[8] I.Clare,[13] R.Clare,[38] G.Coignet,[4] N.Colino,[25] S.Costantini,[39] B.de la Cruz,[25] S.Cucciarelli,[33] J.A.van Dalen,[31] R.de Asmundis,[29] P.Déglon,[20] J.Debreczeni,[12] A.Degré,[4] K.Dehmelt,[26] K.Deiters,[47] D.della Volpe,[29] E.Delmeire,[20] P.Denes,[37] F.DeNotaristefani,[39] A.De Salvo,[49] M.Diemoz,[39] M.Dierckxsens,[2] C.Dionisi,[39] M.Dittmar,[49] A.Doria,[29] M.T.Dova,[10,♯] D.Duchesneau,[4] M.Duda,[1] B.Echenard,[20] A.Eline,[18] A.El Hage,[1] H.El Mamouni,[24] A.Engler,[35] F.J.Eppling,[13] P.Extermann,[20] M.A.Falagan,[25] S.Falciano,[39] A.Favara,[32] J.Fay,[24] O.Fedin,[34] M.Felcini,[49] T.Ferguson,[35] H.Fesefeldt,[1] E.Fiandrini,[33] J.H.Field,[20] F.Filthaut,[31] P.H.Fisher,[13] W.Fisher,[37] I.Fisk,[41] G.Forconi,[13] K.Freudenreich,[49] C.Furetta,[27] Yu.Galaktionov,[28,13] S.N.Ganguli,[9] P.Garcia-Abia,[25] M.Gataullin,[32] S.Gentile,[39] S.Giagu,[39] Z.F.Gong,[22] G.Grenier,[24] O.Grimm,[49] M.W.Gruenewald,[16] M.Guida,[40] R.van Gulik,[2] V.K.Gupta,[37] A.Gurtu,[9] L.J.Gutay,[46] D.Haas,[5] D.Hatzifotiadou,[8] T.Hebbeker,[1] A.Hervé,[18] J.Hirschfelder,[35] H.Hofer,[49] M.Hohlmann,[26] G.Holzner,[49] S.R.Hou,[44] Y.Hu,[31] B.N.Jin,[7] L.W.Jones,[3] P.de Jong,[2] I.Josa-Mutuberría,[25] M.Kaur,[14] M.N.Kienzle-Focacci,[20] J.K.Kim,[43] J.Kirkby,[18] W.Kittel,[31] A.Klimentov,[13,28] A.C.König,[31] M.Kopal,[46] V.Koutsenko,[13,28] M.Kräber,[49] R.W.Kraemer,[35] A.Krüger,[48] A.Kunin,[13] P.Ladron de Guevara,[25] I.Laktineh,[24] G.Landi,[17] M.Lebeau,[18] A.Lebedev,[13] P.Lebrun,[24] P.Lecomte,[49] P.Lecoq,[18] P.Le Coultre,[49] J.M.Le Goff,[18] R.Leiste,[48] M.Levtchenko,[27] P.Levtchenko,[34] C.Li,[22] S.Likhoded,[48] C.H.Lin,[44] W.T.Lin,[44] F.L.Linde,[2] L.Lista,[29] Z.A.Liu,[7] W.Lohmann,[48] E.Longo,[39] Y.S.Lu,[7] C.Luci,[39] L.Luminari,[39] W.Lustermann,[49] W.G.Ma,[22] L.Malgeri,[20] A.Malinin,[28] C.Maña,[25] J.Mans,[37] J.P.Martin,[24] F.Marzano,[39] K.Mazumdar,[9] R.R.McNeil,[6] S.Mele,[18,29] L.Merola,[29] M.Meschini,[17] W.J.Metzger,[31] A.Mihul,[11] H.Milcent,[18] G.Mirabelli,[39] J.Mnich,[1] G.B.Mohanty,[9] G.S.Muanza,[24] A.J.M.Muijs,[2] B.Musicar,[41] M.Musy,[39] S.Nagy,[15] S.Natale,[20] M.Napolitano,[29] F.Nessi-Tedaldi,[49] H.Newman,[32] A.Nisati,[39] T.Novak,[31] H.Nowak,[48] R.Ofierzynski,[49] G.Organtini,[39] I.Pal,[46] C.Palomares,[25] P.Paolucci,[29] R.Paramatti,[39] G.Passaleva,[17] S.Patricelli,[29] T.Paul,[10] M.Pauluzzi,[33] C.Paus,[13] F.Pauss,[49] M.Pedace,[39] S.Pensotti,[27] D.Perret-Gallix,[4] B.Petersen,[31] D.Piccolo,[29] F.Pierella,[8] M.Pioppi,[33] P.A.Piroué,[37] E.Pistolesi,[27] V.Plyaskin,[28] M.Pohl,[20] V.Pojidaev,[17] J.Pothier,[18] D.Prokofiev,[34] J.Quartieri,[40] G.Rahal-Callot,[49] M.A.Rahaman,[9] P.Raics,[15] N.Raja,[9] R.Ramelli,[49] P.G.Rancoita,[27] R.Ranieri,[17] A.Raspereza,[48] P.Razis,[30] D.Ren,[49] M.Rescigno,[39] S.Reucroft,[10] S.Riemann,[48] K.Riles,[3] B.P.Roe,[3] L.Romero,[25] A.Rosca,[48] C.Rosemann,[1] C.Rosenbleck,[1] S.Rosier-Lees,[4] S.Roth,[1] J.A.Rubio,[18] G.Ruggiero,[17] H.Rykaczewski,[49] A.Sakharov,[49] S.Saremi,[6] S.Sarkar,[39] J.Salicio,[18] E.Sanchez,[25] C.Schäfer,[18] V.Schegelsky,[34] H.Schopper,[21] D.J.Schotanus,[31] C.Sciacca,[29] L.Servoli,[33] S.Shevchenko,[32] N.Shivarov,[42] V.Shoutko,[13] E.Shumilov,[28] A.Shvorob,[32] D.Son,[43] C.Souga,[24] P.Spillantini,[17] M.Steuer,[13] D.P.Stickland,[37] B.Stoyanov,[42] A.Straessner,[20] K.Sudhakar,[9] G.Sultanov,[42] L.Z.Sun,[22] S.Sushkov,[1] H.Suter,[49] J.D.Swain,[10] Z.Szillasi,[26,¶] X.W.Tang,[7] P.Tarjan,[15] L.Tauscher,[5] L.Taylor,[10] B.Tellili,[24] D.Teyssier,[24] C.Timmermans,[31] Samuel C.C.Ting,[13] S.M.Ting,[13] S.C.Tonwar,[9] J.Tóth,[12] C.Tully,[37] K.L.Tung,[7] J.Ulbricht,[49] E.Valente,[39] R.T.Van de Walle,[31] R.Vasquez,[46] V.Veszpremi,[26] G.Vesztergombi,[12] I.Vetlitsky,[28] D.Vicinanza,[40] G.Viertel,[49] S.Villa,[38] M.Vivargent,[4] S.Vlachos,[5] I.Vodopianov,[26] H.Vogel,[35] H.Vogt,[48] I.Vorobiev,[35,28] A.A.Vorobyov,[34] M.Wadhwa,[5] Q.Wang,[31] X.L.Wang,[22] Z.M.Wang,[22] M.Weber,[18] H.Wilkens,[31] S.Wynhoff,[37] L.Xia,[32] Z.Z.Xu,[22] J.Yamamoto,[3] B.Z.Yang,[22] C.G.Yang,[7] H.J.Yang,[3] M.Yang,[7] S.C.Yeh,[45] An.Zalite,[34] Yu.Zalite,[34] Z.P.Zhang,[22] J.Zhao,[22] G.Y.Zhu,[7] R.Y.Zhu,[32] H.L.Zhuang,[7] A.Zichichi,[8,18,19] B.Zimmermann,[49] M.Zöller.[1]

1 III. Physikalisches Institut, RWTH, D-52056 Aachen, Germany[§]
2 National Institute for High Energy Physics, NIKHEF, and University of Amsterdam, NL-1009 DB Amsterdam, The Netherlands
3 University of Michigan, Ann Arbor, MI 48109, USA
4 Laboratoire d'Annecy-le-Vieux de Physique des Particules, LAPP,IN2P3-CNRS, BP 110, F-74941 Annecy-le-Vieux CEDEX, France
5 Institute of Physics, University of Basel, CH-4056 Basel, Switzerland
6 Louisiana State University, Baton Rouge, LA 70803, USA
7 Institute of High Energy Physics, IHEP, 100039 Beijing, China[△]
8 University of Bologna and INFN-Sezione di Bologna, I-40126 Bologna, Italy
9 Tata Institute of Fundamental Research, Mumbai (Bombay) 400 005, India
10 Northeastern University, Boston, MA 02115, USA
11 Institute of Atomic Physics and University of Bucharest, R-76900 Bucharest, Romania
12 Central Research Institute for Physics of the Hungarian Academy of Sciences, H-1525 Budapest 114, Hungary[‡]
13 Massachusetts Institute of Technology, Cambridge, MA 02139, USA
14 Panjab University, Chandigarh 160 014, India
15 KLTE-ATOMKI, H-4010 Debrecen, Hungary[¶]
16 Department of Experimental Physics, University College Dublin, Belfield, Dublin 4, Ireland
17 INFN Sezione di Firenze and University of Florence, I-50125 Florence, Italy
18 European Laboratory for Particle Physics, CERN, CH-1211 Geneva 23, Switzerland
19 World Laboratory, FBLJA Project, CH-1211 Geneva 23, Switzerland
20 University of Geneva, CH-1211 Geneva 4, Switzerland
21 University of Hamburg, D-22761 Hamburg, Germany
22 Chinese University of Science and Technology, USTC, Hefei, Anhui 230 029, China[△]
23 University of Lausanne, CH-1015 Lausanne, Switzerland
24 Institut de Physique Nucléaire de Lyon, IN2P3-CNRS,Université Claude Bernard, F-69622 Villeurbanne, France
25 Centro de Investigaciones Energéticas, Medioambientales y Tecnológicas, CIEMAT, E-28040 Madrid, Spain[♭]
26 Florida Institute of Technology, Melbourne, FL 32901, USA
27 INFN-Sezione di Milano, I-20133 Milan, Italy
28 Institute of Theoretical and Experimental Physics, ITEP, Moscow, Russia
29 INFN-Sezione di Napoli and University of Naples, I-80125 Naples, Italy
30 Department of Physics, University of Cyprus, Nicosia, Cyprus
31 University of Nijmegen and NIKHEF, NL-6525 ED Nijmegen, The Netherlands
32 California Institute of Technology, Pasadena, CA 91125, USA
33 INFN-Sezione di Perugia and Università Degli Studi di Perugia, I-06100 Perugia, Italy
34 Nuclear Physics Institute, St. Petersburg, Russia
35 Carnegie Mellon University, Pittsburgh, PA 15213, USA
36 INFN-Sezione di Napoli and University of Potenza, I-85100 Potenza, Italy
37 Princeton University, Princeton, NJ 08544, USA
38 University of Californa, Riverside, CA 92521, USA
39 INFN-Sezione di Roma and University of Rome, "La Sapienza", I-00185 Rome, Italy
40 University and INFN, Salerno, I-84100 Salerno, Italy
41 University of California, San Diego, CA 92093, USA
42 Bulgarian Academy of Sciences, Central Lab. of Mechatronics and Instrumentation, BU-1113 Sofia, Bulgaria
43 The Center for High Energy Physics, Kyungpook National University, 702-701 Taegu, Republic of Korea
44 National Central University, Chung-Li, Taiwan, China
45 Department of Physics, National Tsing Hua University, Taiwan, China
46 Purdue University, West Lafayette, IN 47907, USA
47 Paul Scherrer Institut, PSI, CH-5232 Villigen, Switzerland
48 DESY, D-15738 Zeuthen, Germany
49 Eidgenössische Technische Hochschule, ETH Zürich, CH-8093 Zürich, Switzerland
§ Supported by the German Bundesministerium für Bildung, Wissenschaft, Forschung und Technologie.
‡ Supported by the Hungarian OTKA fund under contract numbers T019181, F023259 and T037350.
¶ Also supported by the Hungarian OTKA fund under contract number T026178.
♭ Supported also by the Comisión Interministerial de Ciencia y Tecnología.
♯ Also supported by CONICET and Universidad Nacional de La Plata, CC 67, 1900 La Plata, Argentina.
△ Supported by the National Natural Science Foundation of China.

$\langle\sqrt{s}\rangle$ [GeV]	188.6	191.6	195.5	199.5	201.8	205.9
Integrated luminosity [pb^{-1}]	176.8	29.8	84.1	83.3	37.2	218.1
$\mathrm{e^+e^-} \to \mathrm{e}\nu\mathrm{q}\bar{\mathrm{q}}$	293	59	133	110	56	355
$\mathrm{e^+e^-} \to \mu\nu\mathrm{q}\bar{\mathrm{q}}$	255	43	110	99	59	289
$\mathrm{e^+e^-} \to \mathrm{q}\bar{\mathrm{q}}\mathrm{q}\bar{\mathrm{q}}$	1447	224	640	683	269	1656

Table 1: Average centre-of-mass energies with corresponding integrated luminosities and numbers of selected events.

	$0.3 < \cos\Theta_{\mathrm{W}^-} < 0.9$				$-0.9 < \cos\Theta_{\mathrm{W}^-} < -0.3$			
	±1 depleted		±1 enriched		±1 depleted		±1 enriched	
	f_-	f_0	f_-	f_0	f_-	f_0	f_-	f_0
Selection	0.034	0.045	0.010	< 0.001	0.053	0.048	0.050	0.087
Fit binning	0.027	0.021	0.030	0.057	0.078	0.097	0.020	0.051
Bias correction	0.018	0.026	0.010	0.013	0.031	0.055	0.016	0.034
Efficiency correction	0.003	0.001	0.005	0.004	0.004	0.006	0.002	0.005
Four fermions	0.001	0.006	0.006	0.003	0.012	0.024	0.003	0.026
Background levels	0.006	0.008	0.004	0.008	0.022	0.024	0.014	0.019
Total	0.048	0.057	0.034	0.059	0.102	0.126	0.058	0.111

Table 2: Systematic uncertainties on the measurement of f_- and f_0 for leptonic W-boson decays in bins of $\cos\Theta_{\mathrm{W}^-}$ and for samples depleted of and enriched in the ±1 helicity. The statistical component of these uncertainties is removed.

	$0.3 < \cos\Theta_{W^-} < 0.9$: $(\lambda_{W^-}, \lambda_{W^+}) = (-1, +1)$ enriched		
	f_-	f_+	f_0
Data ±1 depleted	$0.521 \pm 0.086 \pm 0.048$	$0.121 \pm 0.058 \pm 0.035$	$0.358 \pm 0.116 \pm 0.057$
Data ±1 enriched	$0.839 \pm 0.057 \pm 0.034$	$0.087 \pm 0.034 \pm 0.036$	$0.074 \pm 0.072 \pm 0.059$
Difference	$-0.318 \pm 0.103 \pm 0.059$	$0.034 \pm 0.067 \pm 0.050$	$0.284 \pm 0.137 \pm 0.082$
MC ±1 depleted	0.670 ± 0.008	0.148 ± 0.006	0.182 ± 0.012
MC ±1 enriched	0.781 ± 0.007	0.091 ± 0.004	0.128 ± 0.009
Difference	-0.111 ± 0.011	0.057 ± 0.007	0.054 ± 0.015
	$-0.9 < \cos\Theta_{W^-} < -0.3$: $(\lambda_{W^-}, \lambda_{W^+}) = (0, 0)$ enriched		
	f_-	f_+	f_0
Data ±1 depleted	$0.387 \pm 0.136 \pm 0.102$	$0.398 \pm 0.121 \pm 0.061$	$0.215 \pm 0.316 \pm 0.126$
Data ±1 enriched	$0.152 \pm 0.082 \pm 0.058$	$0.530 \pm 0.101 \pm 0.087$	$0.318 \pm 0.215 \pm 0.111$
Difference	$0.235 \pm 0.159 \pm 0.117$	$-0.132 \pm 0.158 \pm 0.107$	$-0.103 \pm 0.382 \pm 0.168$
MC ±1 depleted	0.186 ± 0.014	0.351 ± 0.016	0.463 ± 0.023
MC ±1 enriched	0.158 ± 0.014	0.532 ± 0.017	0.310 ± 0.026
Difference	0.028 ± 0.020	-0.181 ± 0.023	0.153 ± 0.035

Table 3: The W-boson helicity fractions measured for different intervals of $\cos\Theta_{W^-}$. The results are shown for different subsamples depleted of or enriched in helicity ±1. The corresponding helicity fractions in the Standard Model, as implemented in the KORALW Monte Carlo program, are also given with their statistical uncertainties.

	$f_- - f_0$ correlation coefficient			
	Data		Monte Carlo	
	±1 depleted	±1 enriched	±1 depleted	±1 enriched
$0.3 < \cos\Theta_{W^-} < 0.9$	-92%	-93%	-88%	-91%
$-0.9 < \cos\Theta_{W^-} < -0.3$	-76%	-77%	-80%	-78%

Table 4: Correlation coefficients between the fit parameters f_- and f_0.

	$e^+e^- \to W^+W^- \to \ell\nu q\bar{q}$	$e^+e^- \to W^+W^- \to q\bar{q}q\bar{q}$
Selection	0.013	0.007
Fit binning	0.012	0.007
Efficiency correction	0.001	0.002
Four fermions	0.005	—
Background levels	0.002	0.007
Jet pairing	—	0.011
Total	0.019	0.016

Table 5: Systematic uncertainties on the measurement of the decay-plane correlation parameter D. The statistical component of these uncertainties is removed.

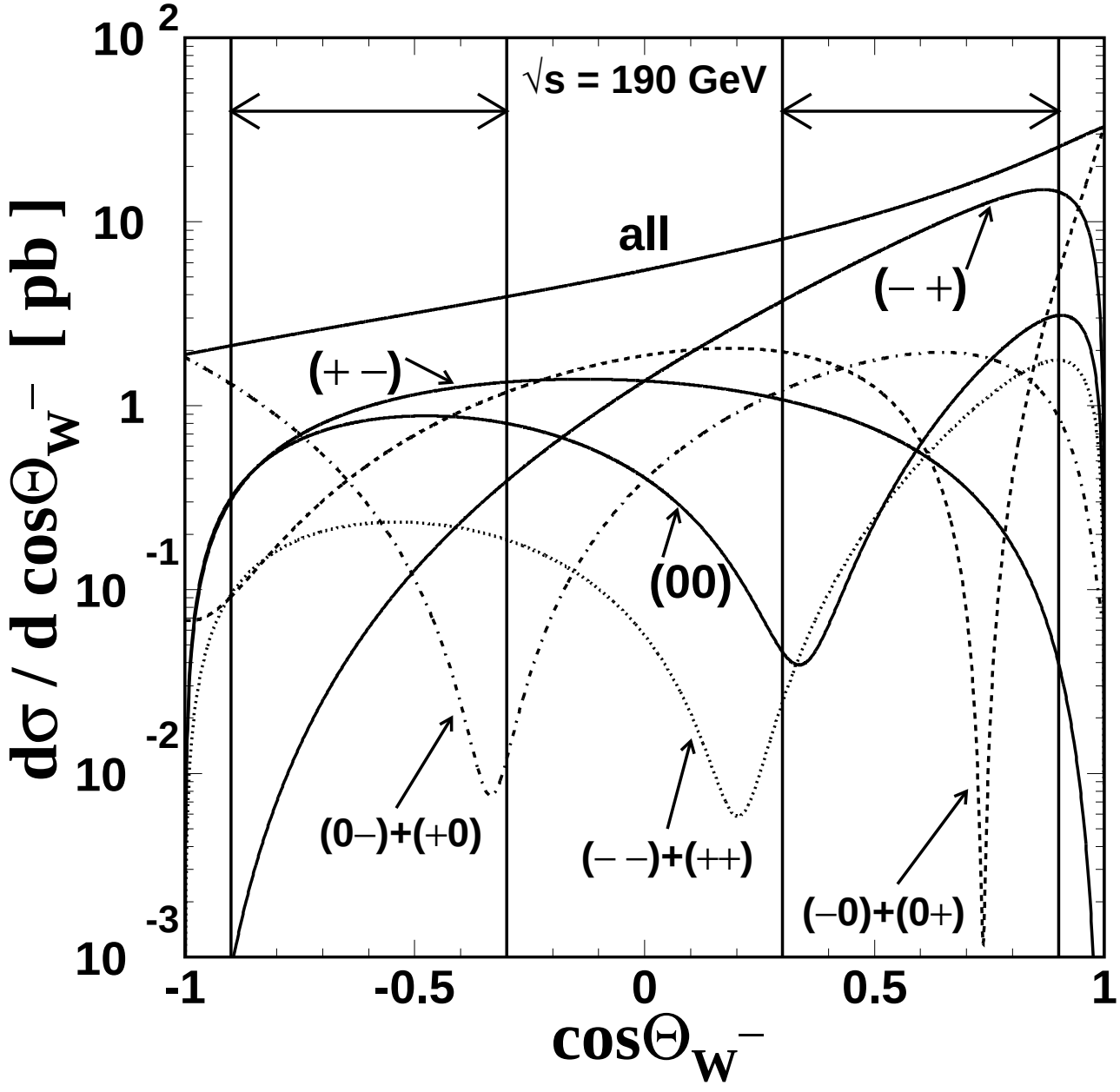

Figure 1: Differential cross section for pair production of polarised W bosons at $\sqrt{s} = 190$ GeV averaged over initial electron polarisations. The W^- and W^+ helicities in the e^+e^- centre-of-mass frame are given in parentheses. The intervals used for the analysis of W-boson spin correlations are indicated by the arrows.

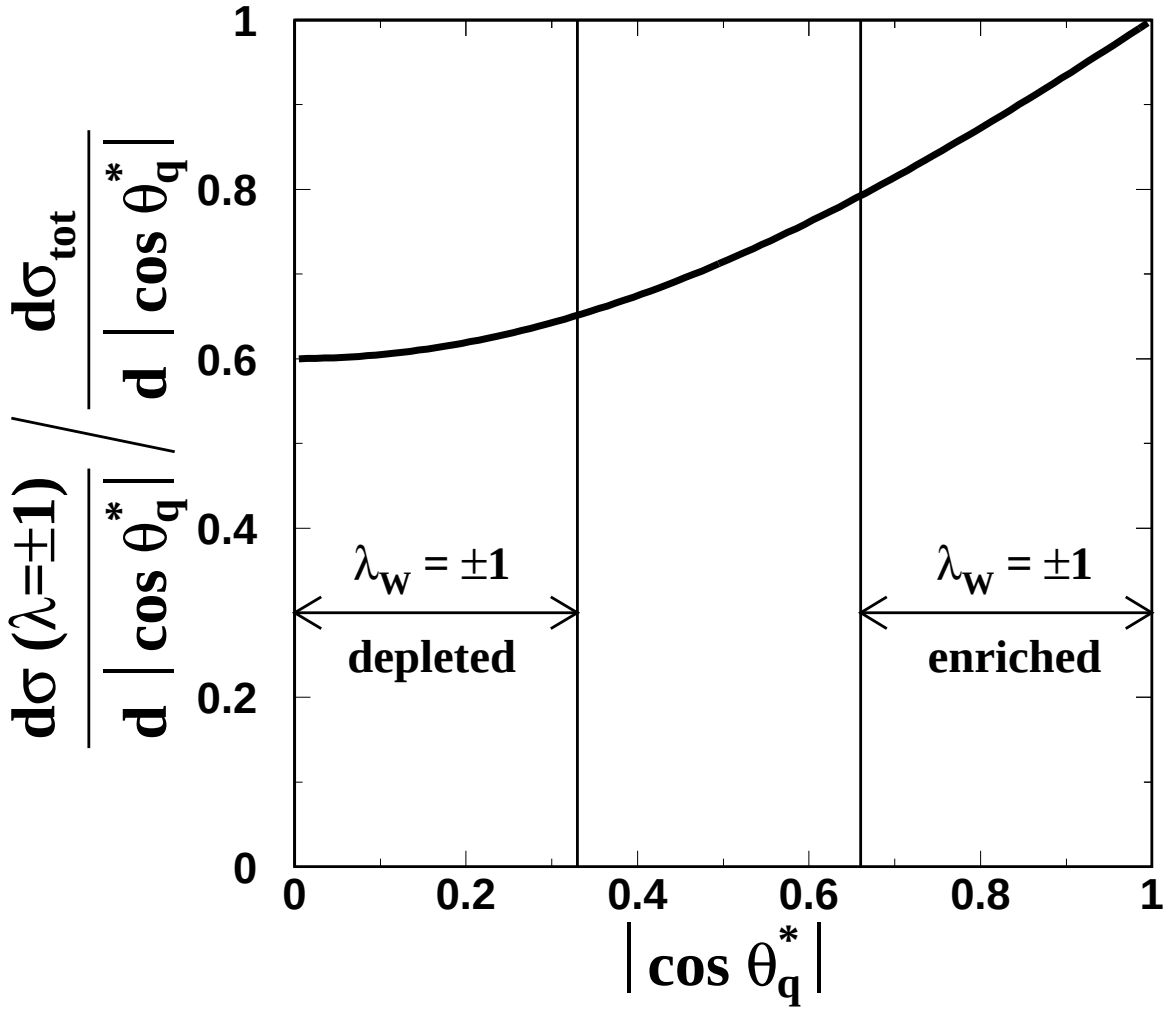

Figure 2: Standard Model predictions for the relative contribution of the helicity states ±1 to the $e^+e^- \to W^+W^- \to \ell\nu q\bar{q}$ differential cross section as a function of $|\cos\theta_q^*|$. The intervals used for the analysis of W-boson spin correlations are indicated.

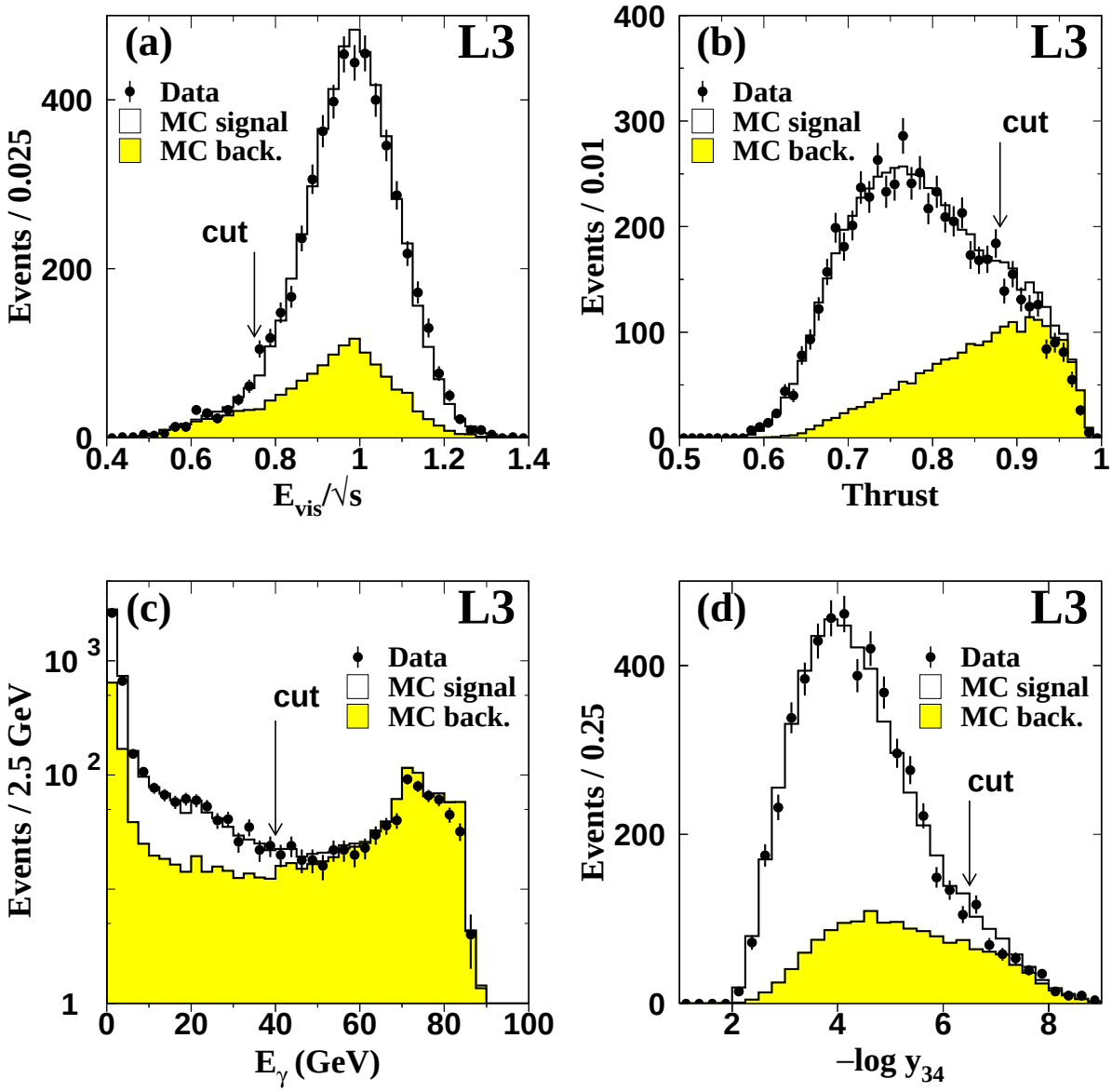

Figure 3: Distributions of variables used for the selection of $e^+e^- \to W^+W^- \to q\bar{q}q\bar{q}$ events: (a) normalised visible energy, (b) event thrust, (c) energy of the most energetic photon, E_γ, (d) jet-resolution parameter, $-\log y_{34}$. In each plot, all other selection criteria are applied. The arrows indicate the positions of the cuts.

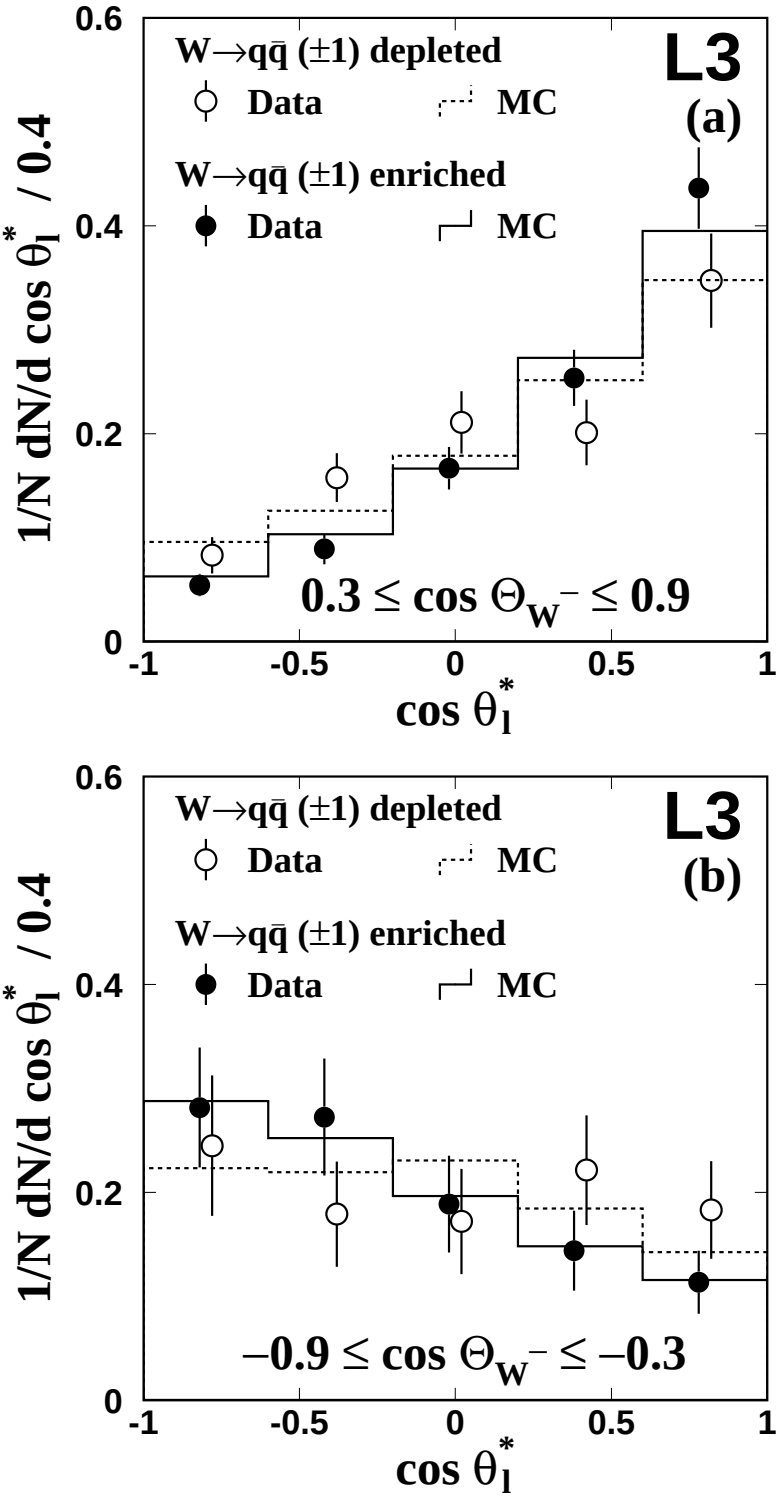

Figure 4: Corrected $\cos\theta^*_\ell$ distributions for $W \to \ell\nu$ decays for data and the KORALW Monte Carlo in the intervals (a) $0.3 < \cos\Theta_{W^-} < 0.9$, and (b) $-0.9 < \cos\Theta_{W^-} < -0.3$. The distributions are shown after classifying the events in two samples, according to the helicity of the W boson decaying into hadrons. The first sample is enriched in W bosons in a transverse-helicity state, the second sample is depleted of W bosons in a transverse-helicity state. For clarity, the data points are slightly shifted.

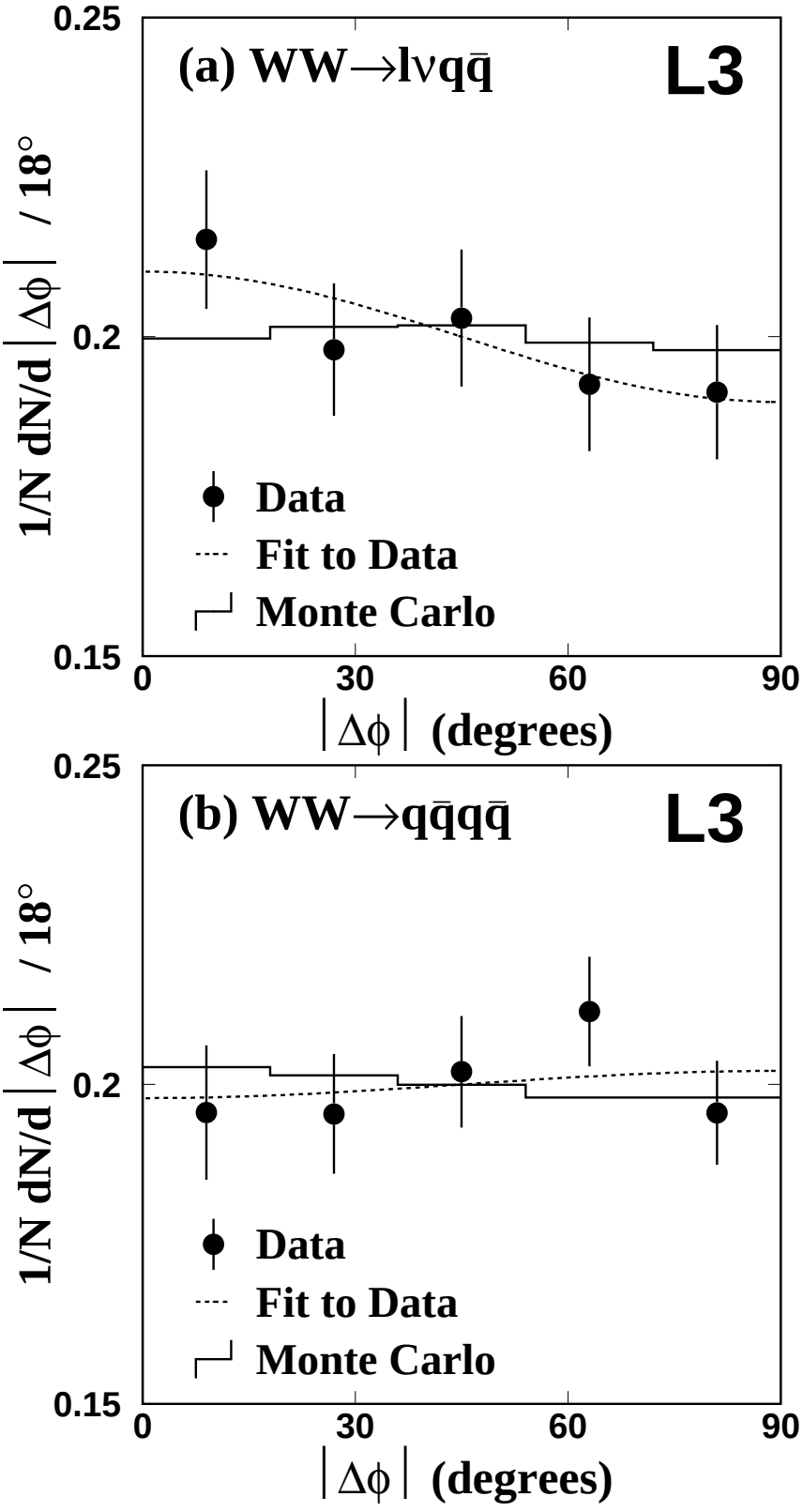

Figure 5: Corrected $|\Delta\phi|$ distributions for (a) $e^+e^- \to W^+W^- \to \ell\nu q\bar{q}$ and (b) $e^+e^- \to W^+W^- \to q\bar{q}q\bar{q}$ events for data and the KORALW Monte Carlo. The fit results are also shown.